Science Advances

AAAS

advances.sciencemag.org/cgi/content/full/1/9/e1500707/DC1

Supplementary Materials for

A surface code quantum computer in silicon

Charles D. Hill, Eldad Peretz, Samuel J. Hile, Matthew G. House, Martin Fuechsle, Sven Rogge, Michelle Y. Simmons, Lloyd C. L. Hollenberg

Published 30 October 2015, *Sci. Adv.* **1**, e1500707 (2015)
DOI: 10.1126/sciadv.1500707

The PDF file includes:

Supplementary Materials

A. Experimental considerations – 3D electrostatic simulations

To understand the level of gate control required for the selective activation/deactivation of individual donor qubits and pairs of adjacent donor qubits, we carried out 3D simulations of the electrostatics of the control structures. The built-in electric field due to the presence of metallic donor gates modifies the Coulombic states raising their ionization energy above the conduction band edge as observed in a single atom transistor [7]. Hence, at zero gate bias all qubits are in the ionised memory state. From the results of the electrostatic simulations we identify the combinations of the voltages applied to S, D and gates (GA, GB, GA′, GB′) at which electrons can be selectively loaded/unloaded from the SET island to activate/deactivate donors at a targeted position, without activating/deactivating neighboring qubits. We also identify bias points for activation of a second qubit for the CNOT gate for donors that both share and do not share an SET island. We find that the voltage control protocols are robust against the positional accuracy achievable with STM lithography, and the voltages applied are kept well within the limits corresponding to the breakdown electric field threshold for Si:P nanostructures [62].

Based on a capacitance matrix calculated from the geometry using the Fastcap capacitance solver [60], we compute the ground state electron occupation numbers for each of the donor qubits and SET islands for different bias configurations using the constant interaction model. The model is purely geometric and does not account for the true quantum mechanical binding energies, but prior experiments have shown this to be an effective qualitative indicator in this type of structure [9]. Current STM lithography techniques allow P donor placement with an accuracy to within 1-2 lattice sites (< 1 nm) [7, 34], so we must consider the effect of the positional uncertainty on electrostatic gate coupling. The electrostatic model indicates that with such a positional uncertainty of ~1 nm only a few percent variation occurs in the coupling capacitances. The uncertainties in the required bias voltages, assuming as much as a 5 nm offset in donor location, are approximately equivalent to the line thickness in the gate-space maps of Figure S1. A breakdown electric field threshold of ~ 10 MV/m has been observed in experiments using monolayer Si:P nanostructures [62]. Therefore, we anticipate a gate pitch between parallel nanowires in each plane of 30 nm will safely allow an operational voltage bias range of ± 250 mV. We show in this section that electrostatic control for one-qubit and two qubit gates can be achieved well within this limitation, opening the possibility for closer qubit placement. In our simulations, the geometry is taken as: Si:P Bohr radius = 2 nm, monolayer gate width = 5 nm, SET island = 13 x 13 nm^2, donor-SET distance = 15 nm, planar gate pitch = 30 nm, and gate layer separation in the vertical direction = 40 nm. The results of the simulations are summarised in Figure S1.

Consider a single SET island (yellow) and its four surrounding donors (red, blue, green and orange), as highlighted in Figure S1(a). A 3D wireframe model used to compute the capacitance matrix is shown in Figure S1(b), where we extend the patterned structures by the Bohr radius in silicon (a_B ~ 2 nm) to represent the extent of the electronic wave function [55, 56]. In the model we include SET cells surrounding the one of interest, out to next nearest neighbours to avoid boundary effects. Additional electrons are provided to the system of 5 charge structures in the model (SET and 4 donors) from the source and drain nanowires labelled S and D. By applying a negative voltage to the S and D lines, we plunge the electrochemical potential of the SET and donors relative to the metallic Fermi levels of S and D (which are offset by a small bias voltage V_{SD} ~ 1 mV across the SET to provide a measurable readout current). The result can be seen in the simulated gate-space map of Figure S1(c). In Figure S1(c) the plunge and tilt voltage axes represent the following combinations of bias voltages on the control lines:

$$V_{\text{plunge}} = V_S - V_{SD} = V_D$$
$$V_{\text{tilt}} = 2V_{GA} = -2V_{GA'} = V_{GB} = -V_{GB'}$$

Here as we reduce V_{plunge} from 0 V we add additional electrons to the SET each time we cross the yellow lines (I, II, III). Moving down along the left edge, each yellow line indicates an additional electron being added to the SET (marked I, II). With nothing to discriminate the energy levels of the four donors as V_{plunge} passes –15mV (marked III where the red, blue, green and orange lines meet) all the donors would gain an electron. In order to select a particular donor for loading, we have to tilt the potential landscape surrounding the SET to offset their loading potentials by biasing the four surrounding control lines (GA, GB, GA′, GB′). With increasing voltage, the loading lines for the four donors separate so that we can preferentially load an electron onto any individual donor with voltages well inside the ± 250 mV limit. The order of the separated load potentials can be modified to select whichever donor we choose by permuting the polarity and strength of each gate in the definition of V_{tilt}. Readout and load/unload procedures are executed around an inter-dot (SET-donor) triple point, for example the intersection of yellow and red lines (marked IV). During ESR and NMR pulses, voltages should be moved away from the transition lines into Coulomb blockade to ensure qubit configurations are locked.

Figure S1(d) indicates the operating region for a single qubit gate on the red donor. The requirement is simply that the red donor is occupied (active qubit state) and all other surrounding donors remain ionized (memory qubit state) – this Coulomb blockaded configuration corresponds to the red shaded area. Beyond the blue line the donor marked as blue will also load, and within the grey regions multiple other unwanted donors become activated. Since single qubit operations activate only 3 horizontal (GB, D, GB′) and 3 vertical (GA, S, GA′) nanowires, this red region confirms that single qubit gates can be controlled and run simultaneously in parallel on numerous other donors beyond those surrounding nearest neighbour SETs.

From an electrostatic perspective there are two classes of two-qubit configurations, which we label as Type-I and Type-II. Those between donors who share a single SET (Type-I: blue and red in Figure S1(a)), and those between donors that do not share an SET (Type-II: purple and red in Figure S1(a)). In the first case (Figure S1(d)), the requirements for the CNOT gate can be met by loading the red donor at its triple point (marked IV), moving into Coulomb blockade in the red shaded area to apply ESR on the CNOT-target electron, loading the blue CNOT-control qubit at its triple point (marked V), and then moving into the blue shaded blockade region, where the dipole-dipole interaction is present, for all remaining ESR and NMR pulses. Importantly this simulation shows that the CNOT- target donor is not ionised at any point during further qubit donor operations. To achieve the same stability for the second class of interacting qubit pairs (Type-II), we must adjust the definition of V_{plunge}. To access the purple qubit loading potential, we additionally plunge the potential of the western neighbour SET with the neighbouring drain line (marked D′ in Figure S1(a)), but by a lesser amount than for the first drain line (D). We plot in Figure S1(e) the effect of this dual plunge with $V_{dualplunge} = V_S = V_D = 2.2V_{D'}$, where the factor 2.2 is such that the purple donor readout triple point (marked VI) falls between the red and blue qubit loading lines. This facilitates the two-qubit CNOT gate on the red/purple pair, without loading the blue donor or any other. Here the dipole interaction is present within the red/purple hashed shaded region.

We anticipate that optimisations to this basic biasing scheme are possible; however, importantly these simulation results indicate that the proposed scheme is viable with modest voltages and is robust against small variations in capacitive coupling.

B. Phase-matched (PM) qubit activation/deactivation

Having established that the criss-cross array provides sufficient electrostatic control over individual donors to activate/deactivate qubits, we now consider these operations from the standpoint of the

quantum information encoded on the donor nuclear spin. The PM load/unload protocol is described schematically in Figure S2. Figure S2(a) indicates the relevant gate bias conditions on the charge stability map around the donor-SET interdot transition. Solid green and pink lines represent the loading potentials for spin-down and spin-up electrons respectively, and yellow lines the condition for current to flow through the vertical SET at the degeneracy point between n and n + 1 electron occupancy states. Figure S2(b) outlines the phase matched pulse scheme, showing how the system is moved between the marked (and colour-coded) positions for memory, loading, unloading and readout operations, and the details of the state configuration at each position are represented in panels (c)-(f). Between operations, donors are kept idle in the memory configuration (Figure S2(c)). Here the SET is occupied by n electrons; the source and drain Fermi levels (offset by a small bias V_{SD}) are between the $n-1 \leftrightarrow n$ transition (lower solid yellow line) and $n \leftrightarrow n+1$ transition (upper solid yellow line), and also below the donor potential (both Zeeman states are shown). The PM load begins by moving to the 'Load' configuration (Figure S2(e)) for a time Δt. In this arrangement of energy levels an electron may move from source to SET to drain and SET current flows (pink dashed arrows), since the $n \leftrightarrow n+1$ potential lies within the source-drain bias window. Assuming a strongly coupled SET, the timescale for this process is fast compared to Δt, so the n + 1 SET state is occupied with high probability as indicated by hashed shading up to the resonant transition. The characteristic tunnel time from SET to donor is, however, slow compared to Δt, so although filling of the spin-down donor state is energetically allowed (blue arrow), it is improbable during the first load pulse. The system is next pulsed to the 'Active' configuration (Figure S2(f)), and held there until the next phase-matched time window. Assuming the donor has not yet loaded, the additional SET electron will quickly tunnel out to source or drain since it is positioned above the Fermi energy. The 'Load' and 'Active' phases repeat and at some time during a 'Load' phase (Figure S2(e) again) an electron will move from SET to donor. Note that only the spin-down state is accessible due to Zeeman splitting. The SET size we propose is in the regime of small orbital energy separation [63], providing electrons of both spin at the SET's Fermi level. The discrete lines in the diagram represent only the electrostatic charging energy. Once the donor is loaded with one electron, there is an additional mutual charging energy which raises the SET potential to the dotted line, which sits above the level of the source and drain Fermi energy, hence the SET current is thus effectively switched off. Importantly, the 'Active' configuration (Figure S2(f)) is stable also once the donor is loaded. This relies on the charging energy of the SET, which prevents the donor electron from tunnelling back to the SET. At the completion of the PM load operation, the qubit is kept in the 'Active' configuration for all ESR and NMR driven spin manipulations. The PM unload proceeds in a similar way, switching between 'Unload' (Figure S2(d)) and 'Memory' (Figure S2(c)) positions. In a similar way to the 'Active' state, the memory configuration is stable both when the donor is occupied and when it is not, so we are not concerned that probabilistically it takes many 'Unload' cycles before the electron will tunnel out to the SET.

Electron readout occurs with the same state configuration as for 'Load' as shown in Figure S2(b). For a 'Read' operation however, we are no longer concerned with preserving the phase of the underlying nuclear spin, and perform a simple one-step 'Read' (Figure S2(e)) with a duration longer than the tunnel rate. A spin-up electron will tunnel to the SET (pink arrow), removing the mutual charging energy, and switching on the SET current for some time before a spin-down electron re-occupies the donor switching the SET back off. This short-lived current response is the signal indicating measurement of a spin-up state, and does not occur if the electron is projected as spin-down. The readout is followed by a single 'Unload' step to ensure the donor is ionised before returning to the 'Idle' state.

Supplementary Materials figure titles and captions

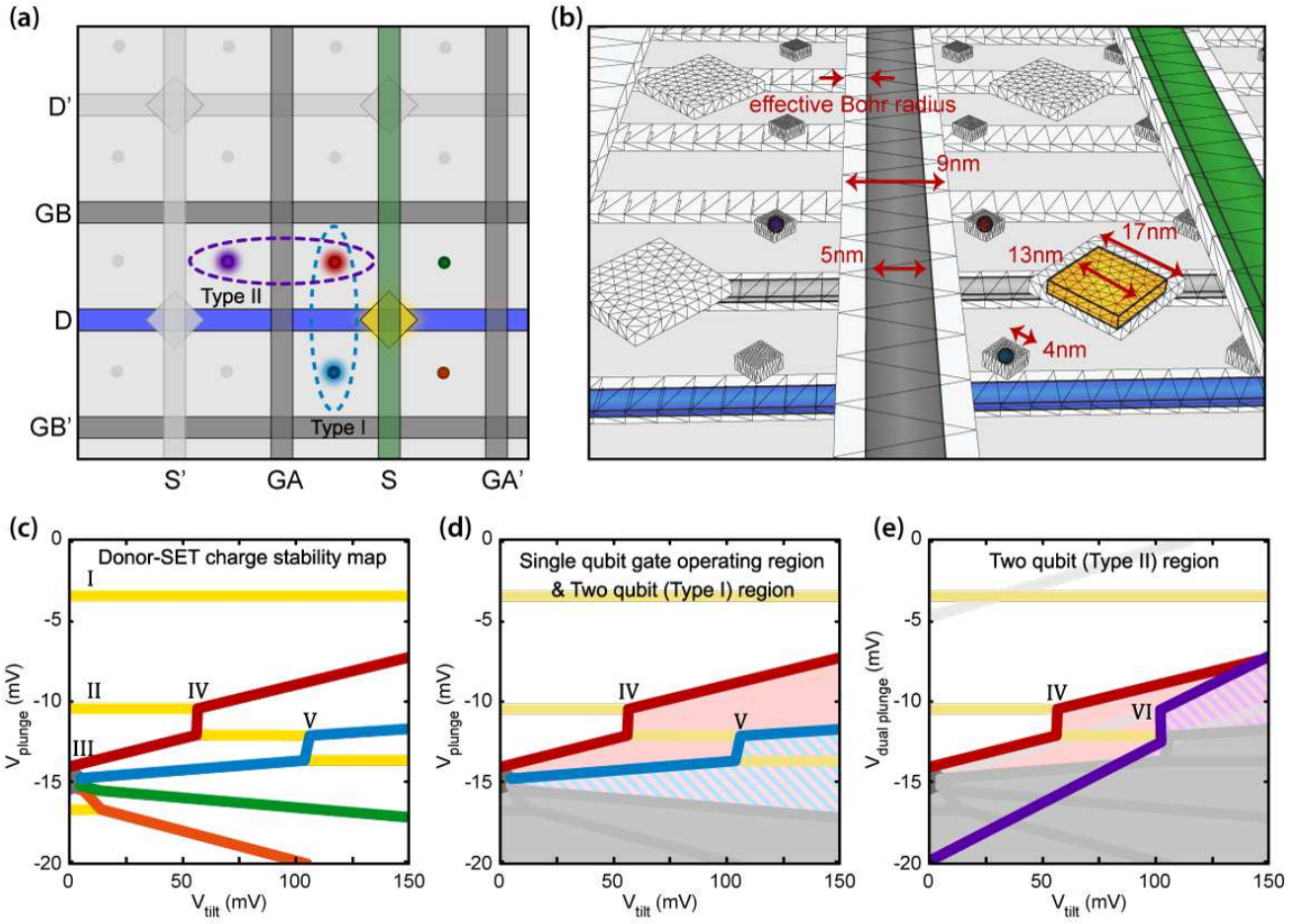

FIG. S1: 3D electrostatic simulations of gate control for qubit addressing.

(a) Overview: A pair of source (S) and drain (D) leads crossing an SET are negatively biased to plunge the loading potentials of its four nearest donors. The symmetry in the four donor potentials is broken by a detuning combination of (GA,GB, GA', GB') that allow a single donor to be selected for electron loading. (b) 3D wireframe model used for Fastcap capacitance computation. The spatial extent of all entities is dilated by 2 nm in all directions consistent with the Bohr radius in silicon. (c) Charge stability analysis: Increasingly negative $V_{plunge} = V_S = V_D$ loads additional electrons to the SET (yellow lines I and II). At $V_{plunge} = 15$ mV, $V_{tilt} = 0$ an electron is loaded in any one of four donors (III). A voltage V_{tilt} along the x-axis separates the loading conditions for the donors (colour coded). In this case $(V_{tilt} = 2V_{GA} = -2V_{GA'} = V_{GB} = -V_{GB'})$ the red donor is loaded preferentially. Spin selective load and readout occurs at the intersection of donor and SET lines at IV, V etc. (d) Gate coordinates (red shaded region) where only the red donor is occupied and all others surrounding it are ionised. The blue hashed region indicates coordinates where additionally its south neighbour (blue) is loaded as for a two qubit gate. Greyed out areas indicate that other targeted donors are loaded. (e) Non-shared SET case (Type II): A two-qubit gate on the red and purple donors requires adding a plunge voltage to the neighbouring drain $V_{dualplunge} = V_S = V_D = 2.2V_{D'}$. This allows sequential and selective loading of just those two donors.

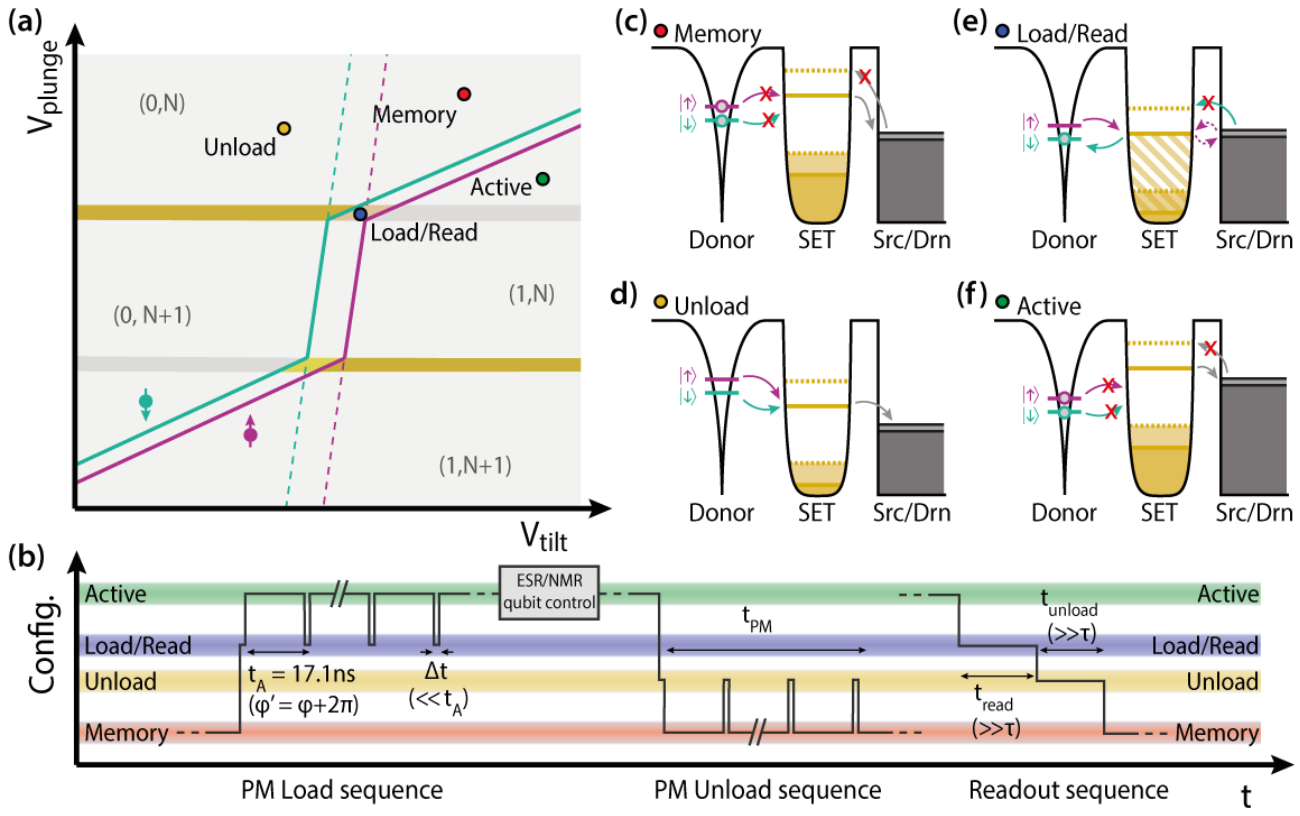

FIG. S2: Implementation of the PM activation/deactivation sequence.

Figure (a) shows schematically the location of the required bias points on a charging diagram corresponding to memory (idle), active, load, unload and readout configurations. A load/control/unload/read sequence is shown in figure (b) in which voltages are pulsed to only allow tunnelling between SET island and donor at times which are phase locked to the hyperfine frequency to prevent unknown phase accumulation on the nuclear spin. The other figures detail these configurations: Figures (c) through (f) show schematics of the chemical potential of donor, SET island and S/D lines for each case: the memory (idle), load/read, unload and active configurations. Dotted lines indicate the SET transition potentials when an electron is present on the donor, and solid lines indicate transition potentials when the donor is ionized.